Article ID: 1006-8775(2017) 02-0146-09

STUDY ON THE MULTIVARIATE STATISTICAL ESTIMATION OF TROPICAL CYCLONE INTENSITY USING FY–3 MWRI BRIGHTNESS TEMPERATURE DATA

ZHANG Miao (张 淼), QIU Hong (邱 红), FANG Xiang (方 翔), LU Nai-meng (卢乃锰)
(Key Lab of Radiometric Calibration and Validation for Environmental Satellites, China Meteorological Administration (LRCVES/CMA) and National Satellite Meteorological Center, Beijing 100081 China)

Abstract: A technique for estimating tropical cyclone (TC) intensity over the Western North Pacific utilizing FY-3 Microwave Imager (MWRI) data is developed. As a first step, we investigated the relationship between the FY-3 MWRI brightness temperature (TB) parameters, which are computed in concentric circles or annuli of different radius in different MWRI frequencies, and the TC maximum wind speed (Vmax) from the TC best track data. We found that the parameters of lower frequency channels' minimum TB, mean TB and ratio of pixels over the threshold TB with a radius of 1.0 or 1.5 degrees from the center give higher correlation. Then by applying principal components analysis (PCA) and multiple regression method, we established an estimation model and evaluated it using independent verification data, with the RMSE being 13 kt. The estimated Vmax is always stronger in the early stages of development, but slightly weaker toward the mature stage, and a reversal of positive and negative bias takes place with a boundary of around 70 kt. For the TC that has a larger error, we found that they are often with less organized and asymmetric cloud pattern, so the classification of TC cloud pattern will help improve the acuracy of the estimated TC intensity, and with the increase of statistical samples the accuracy of the estimated TC intensity will also be improved.

Key words: tropical cyclone intensity; multivariate statistical estimate; FY-3; microwave imager
CLC number: P444 **Document code:** A
doi: 10.16555/j.1006-8775.2017.02.003

1 INTRODUCTION

The tropical cyclone (TC) is the weather system that causes severe disaster to the society by bringing strong wind and heavy rainfall. Thus, it is important to develop an estimation technique of TC intensity for disaster mitigation and prevention. Over the ocean where conventional meteorological data are very scarce, satellites provide the most common means for monitoring these storms. Most operational centers estimate TC intensity by the "Dvorak technique" [1, 2], which is based on a "pattern recognition" of satellite visible and infrared imagery, and is generally successful [3]. However, it is difficult to detect the low-level characteristics of TC when the upper-level is masked by a dense cirrus canopy, while microwaves can penetrate most clouds beyond the top layer and delineate the internal feature of TCs [4, 5]. The ability of satellite-borne passive microwave radiometers to detect the TC has been demonstrated in many studies, such as Niu et al.[6], who used TRMM/TMI data to quantitatively analyze the relationship between precipitation, water vapor path, and latent heat of tropic cyclones over the Northwest Pacific Ocean, Wang et al. [7] used the microwave brightness temperature (TB) data from TRMM/TMI to retrieve the precipitation of typhoon Aere.

Satellite-borne passive microwave temperature sounders have been used to monitor the TC intensity by many scholars. In summary, the 55-GHz region of microwave observations of TC upper tropospheric warm anomalies are linked to the TC intensity [8–11]. Recently, satellite-borne passive microwave imagers were also used to monitor the TC intensity. Initially, only the 85-GHz channel was utilized [12–14] because of its high resolution and sensitivity to precipitation-sized ice particles, which are produced from strong updrafts, and accompanied with these updrafts, the release of latent heat provides TC the energy required for development and maintenance. Therefore studies have related information from 85 GHz to TC intensity, future intensity, and intensity change with varying degrees of success[12–14]. Then some other studies develop a method for TC intensity estimation using not only high-frequency data sets but also low-frequency channels, such as in the work of Hoshino et al.[15] who developed a TC intensity estimation method utilizing

Received 2015-09-02; **Revised** 2017-04-22; **Accepted** 2017-05-15
Foundation item: National Key Research and Development Program of China (2016YFA0600101); National Basic Research Program of China (973 Program, 2010CB950802); National Natural Science Fund (41605028)
Biography: ZHANG Miao, M.S., primarily undertaking research on satellite meteorology.
Corresponding author: QIU Hong, e-mail: qiuhong@cma.gov.cn

10-, 19-, 21-, 37- and 85-GHz channels of TRMM/TMI. As a first step, they computed the TB parameters in concentric circles or annuli of different radius in different TMI frequencies, then after choosing three parameters out of 30 candidates, they computed the regression coeffficients and chose 10 regression equations, sorted by lower root mean square error (RMSE), and then adopted the mean value of the ten as the final estimated Vmax. Yoshida et al.[16] adopted the same technique of Hoshino to estimate the TC intensity using microwave imagery from AMSR-E (Advanced Microwave Scanning Radiometer-Earth Observing Systerm), which also utilized the low-frequency channels.

Launched on November 5, 2010, the FY-3 weather satellite is the 2nd generation of China's polar-orbit weather satellites, and the Microwave Radiation Imager (MWRI) is one of its main payloads. Utilizing the data from 2011 –2013, we investigated the relationship between the FY-3B MWRI TB parameters and the TC Vmax from the TC best track data, and then by applying principal components analysis (PCA) and multiple regression method, we established an estimation model for estimating TC intensity over the Western North Pacific.

2 RELATIONSHIP BETWEEN TB PARAMETERS AND TC VMAX

2.1 *Data*

FY-3B MWRI has ten channels at 10.65, 18.7, 23.8, 36.5 and 89.0 GHz with dual polarization. The characteristics of channels are presented in Table 1. The MWRI/L1 TB data are available from National Satellite Meteorological Center (NSMC), and can be downloaded via the web at http://satellite.cma.gov.cn/portalsite/default.aspx. The TC best track data are available from Japan Meteorological Agency (JMA), and can be downloaded via the web at http://www.jma.gov.jp/jma/jma-eng/jma-center/rsmc-hp -pub-eg/ besttrack. html.

Table 1. Characteristics of MWRI channels.

Frequency (GHz)	10.65	18.7	23.8	36.5	89
Polarization	V, H	V, H	V, H	V, H	V, H
Bandwidth(MHz)	180	200	400	900	4600
Resolution (km×km)	85×51	50×30	45×27	30×18	15×9

2.2 *Theory*

The horizontal polarized TB images of FY-3B MWRI on LEKIMA (28th typhoon of 2013) are shown in Fig.1, and visible and infrared images of Visible and InfraRed Radiometer (VIRR) close to the microwave observations are shown in Fig.2. It can be seen that compared with the visible and infrared observation, microwave images can reveal the precipitation clouds of the TC, especially the deep convective clouds at the eyewall and the outside rainband.

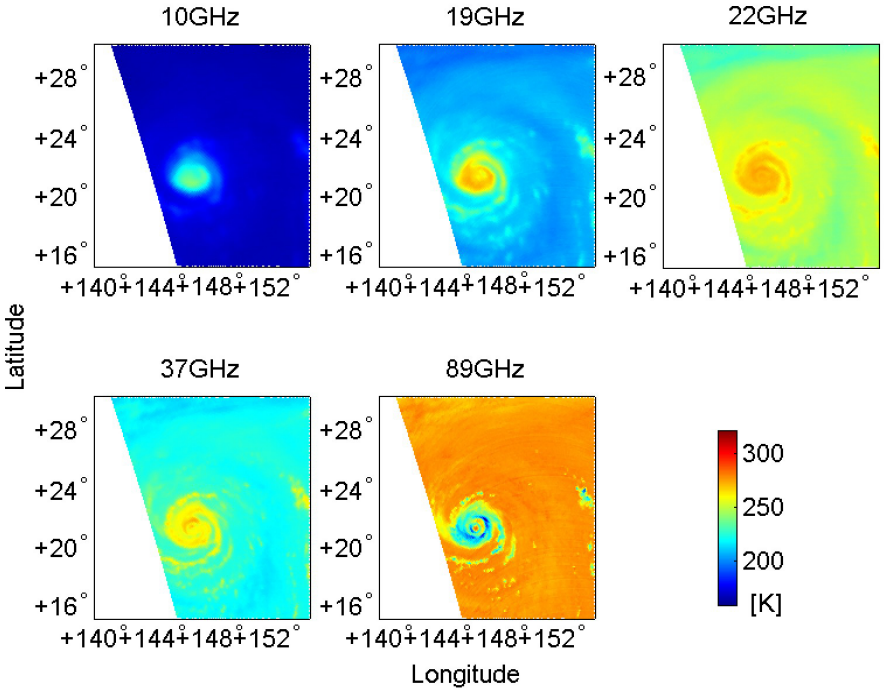

Figure 1. Horizontal polarized TB images of FY-3B MWRI on LEKIMA at 03:05 UTC, 24 October, 2013.

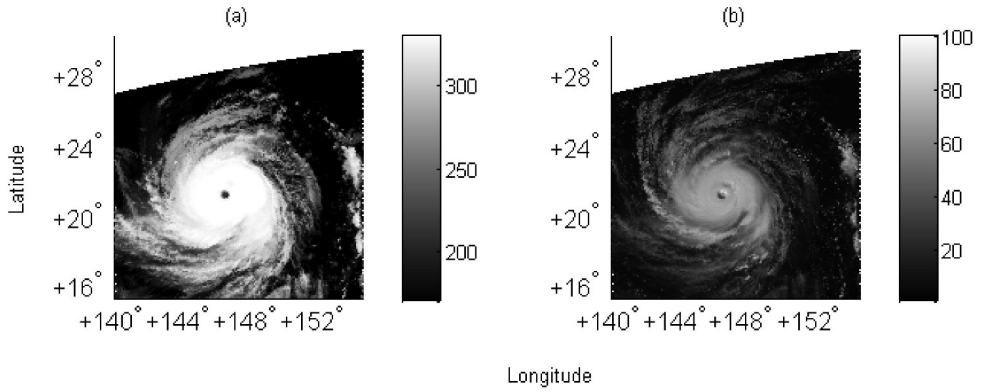

Figure 2. Infrared (a) and visible (b) images of VIRR on LEKIMA at 03:35 UTC, 24 October, 2013.

Using the basic atmospheric parameters of Hurricane Katrina performed by the University of Wisconsin's Non-hydrostatic Modeling System (UW-NMS) cloud resolving model[17] in conjunction with the VDISORT microwave radiative transfer model [17], we simulated the upwelling TB, and preliminarily analyzed the response of MWRI channels to the columnar liquid/ice water content (CWC) of the five hydrometeors (rain drops, snow, graupel particles, cloud droplets and pristine ice crystals) used in the model. A cross-section of this simulation are shown in Fig.3. We can see that close to the center of the hurricane, the TB of lower frequencies (the 10.65, 18.7 and 23.8 GHz) gets higher as the hydrometeors increase, and at the 37-GHz channel and with less hydrometeors, the TB gets higher as the hydrometeors increase; with more hydrometeors, due to the scattering of the hydrometeors (especially snow and graupel), the TB gets lower as the hydrometeors increase, and the TB of the 89-GHz channel gets lower as the hydrometeors increase.

Based on the observation and simulation analysis above, we concluded that the mean, mimimun, maximum TB, and ratio of pixels over the threshold TB, which are computed in concentric circles or annuli of different radius in different MWRI frequencies, can be used to estimate the TC intensity.

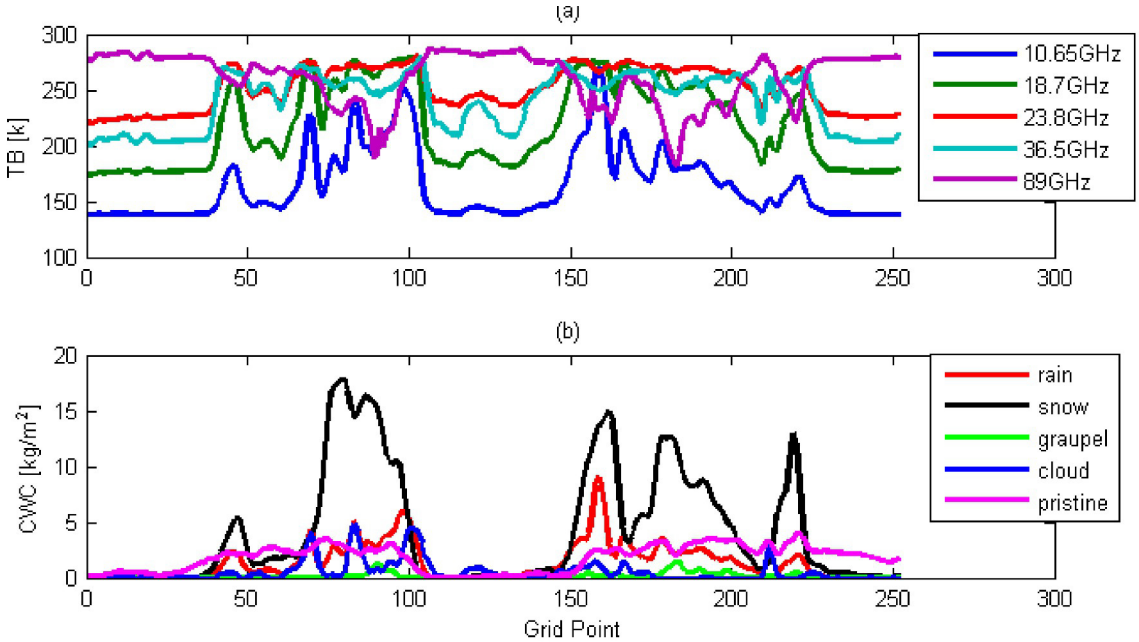

Figure 3. Cross sections of Hurricane Katrina simulation showing the TB of MWRI channels (a), and the CWC of the five hydrometeors (b).

2.3 *Methodology*

In this study, we investigated TCs which developed to the tropical strom stage (when maximun wind speed is over 35 kt) over the Western North Pacific, and cases having land within a 2° concentric circle of the TC center were excluded. Then the number of cases in 2011, 2012, 2013 are 43, 73 and 80 separately, the center location of these cases are shown in Fig.4.

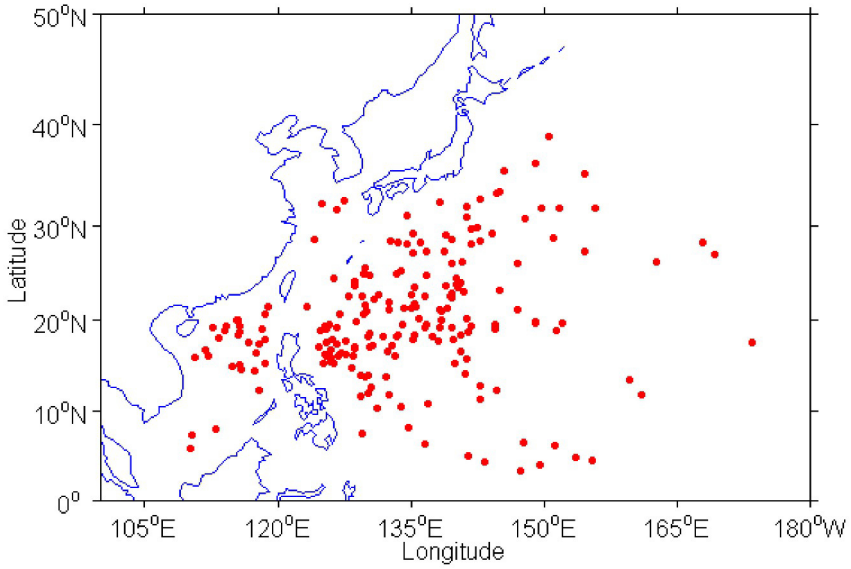

Figure 4. The center location of TCs.

Following Hoshino et al. [15], the parameters are computed by selecting the frequecy, coverage and type of computation. Two choices were used for the selection of coverage. One is a concentric circle, with different radius every 0.5° latitude to 2° latitude. Another is an annuli enclosed by circles every 0.5° latitude. The mean (MEAN), minimum (MIN), maxmum (MAX) TB, and ratio of pixels over the threshold (AREA) TB are computed in the computation-covered area. For AREA, a parameter is computed every 10 K threshold[15], as shown in Table 2. According to this method, 1,050 parameters are obtained. Hereafter, each parameter is named as follows: First, frequecy is presented (e.g., TB10H for horizontal polarized TB of 10 GHz), or PCT (Polarization Corrected Temperature) 89 (PCT89= $1.818TB_V - 0.818TB_h$[15], TB_V is the horizontal polarized TB of 89 GHz and TB_h is the vertical polarized TB of 89 GHz). Second, a type of parameter (i e., MEAN, MIN, MAX, AREA). For AREA, a threshold number follows. Finally, a type of computation coverage (C or A) follows. The computation region is written as 'C', followed by radius for circles, and 'A', followed by inner radius and outer radius for annuli. For example, 'C10' represents a circle whose radius is 1.0° latitude and 'A1015' represents annulus whose inner radius is 1.0° latitude and outer radius is 1.5° latitude. Thus, 'TB10H_MEAN_C10' denotes the mean TB of 10 GHz-H in circle of 1.0° latitude radius.

Table 2. The minimum and the maximum threshold temperatures for each frequency channels and PCT89.

Frequency	Minimum [K]	Maximum [K]
10 GHz	110	200
19 GHz	190	260
21 GHz	190	270
37 GHz	210	270
PCT89	180	270

2.4 *Results*

We computed the correlation coefficients (Corr. Coef.) between the TB parameters and the Vmax from the best track data, and the t test with significance levels of α=0. 05 is conducted. 792 parameters passed the t test, and will be used in the next section. The highest three correlated parameters of lower frequency channels and PCT89's MIN, MAX, MEAN, AREA parameters with the Vmax are shown in Table 3. Corr. Coef. are also given. The following characteristics are inferred from it:

The Corr. Coef. of lower frequecies are higher than PCT89. At lower frequecies there is enhanced sensitivity for liquid water paths in the range from about 0 to 0.5 mm. This range is represented often in the water-laden core regions of TC [18]. However, the 85-GHz channel saturates in amounts greater than about 0.3 mm[14], so the lower frequecies can better reflect the structure of TC.

The MIN (MAX for PCT89), AREA and MEAN of lower frequecies are highly correlated with the Vmax, but MAX (MIN for PCT89) of lower frequecies show lower correlation. The TB at lower frequecies gets higher and PCT89 gets lower as hydrometeors increase, indicating the same trend as an organized TC proceeds. This suggests that MAX (MIN for PCT89) of lower frequecies should be highly correlated with the Vmax, but the result is not the case. The possible reason is that MAX is likely to be high even when there is a small active convection, or a few pixels with heavy rainfall in the region, but it does not represent the TC's overall intensity [16]. In addition, the effect of attenuation and scattering with hydrometeors affects the TB to sature in the TC as the hydrometeors increase. So the MIN

(MAX for PCT89), AREA and MEAN of lower frequecies represent the TC's overall intensity better.

For the parameters of lower frequecies, the high correlation with the Vmax is in C10 and C15. We speculate that the overall TC intensity is not only related with the core region, but also the surrounding region. Of course, this may be related with the average size of eyes or the TCs [16], so we might have to consider the size of eyes or the TCs in the future work.

Table 3. The highest three correlated parameters of lower frequency and PCT89's MIN, MAX, MEAN, AREA parameters with the Vmax, and the Corr. Coef.

Parameter	Corr. Coef.	Parameter	Corr. Coef.
TB19H_MIN_C10	0. 7823	PCT89_ MIN_C05	–0. 2561
TB37H_MIN_C10	0. 7726	PCT89_MIN_A1015	–0. 1615
TB19V_MIN_C10	0. 7702	PCT89_MIN_A1020	–0. 1512
TB10V_MAX_C05	0. 5690	PCT89_MAX_A0510	–0. 6626
TB10V_MAX_C10	0. 5058	PCT89_MAX_A0515	–0. 6024
TB10h_MAX_A0510	0. 4721	PCT89_MAX_A1015	–0. 5850
TB10V_MEAN_C10	0. 7656	PCT89_MEAN_C20	–0. 6111
TB10V_MEAN_C15	0. 7601	PCT89_MEAN_C15	–0. 6047
TB10H_MEAN_A0510	0. 7575	PCT89_MEAN_A0520	–0. 6023
TB10H_AREA160_C10	0. 7904	PCT89_AREA260_A0515	–0. 6506
TB10H_AREA170_C10	0. 7757	PCT89_AREA260_C15	–0. 6480
TB10H_AREA160_A0510	0. 7720	PCT89_AREA270_C20	–0. 6463

3 ESTIMATION OF VMAX USING PCA AND MULTIPLE REGRESSION METHOD

3.1 *Methodology*

The parameters are too many to be easy to have a significant linear correlation between each other on the one hand, and using the stepwise regression method to establish an estimation model may cause instability problems on the other. Therefore, this study utilized the PCA method [19]. PCA is a statistical procedure that uses an orthogonal transformation to convert a set of observations of possibly correlated variables into a set of values of linearly uncorrelated variables, called principal components. The number of principal components is less than or equal to that of the original variables. This transformation is defined in such a way that the first principal component has the largest possible variance (or, accounts for as much of the variability in the data as possible), and each succeeding component in turn has the highest variance possible under the constraint that it is orthogonal to (i.e., uncorrelated with) the preceding components. By using only the first few principal components, the dimensionality of the transformed data is reduced, and the instability is effectively restrained.

The data in 2011 and 2012 are used to develop the TC intensity estimation method. The main principal components' cumulative variance contribution are shown in Table 4. As can be seen that the cumulative variance contribution of the first seven principal components can reach above 90%, the first seven principal component are used as new parameters to compute the regression equation,

$$\hat{f} = a_0+a_1z_1+a_2z_2+a_3z_3+a_4z_4+a_5z_5+a_6z_6+a_7z_7$$

where $\hat{f}$ is the estimated Vmax, z is the new parameters, and a is the regression coefficients, which are shown in Table 5.

Table 4. The main principal components'cumulative variance contribution.

number	1	2	3	4	5	6	7	8	9	10
	53.0%	76.6%	82.8%	85.7%	88.0%	89.7%	91.1%	92.0%	92.7%	93.4%

Table 5. Regression coefficients using the data of 2011 and 2012 as the statistical samples.

a_0	a_1	a_2	a_3	a_4	a_5	a_6	a_7
21.0793	0.0410	–0.0070	0.0095	0.0290	0.0448	0.0046	0.0079

3.2 *Verification*

The independent verification data during 2013 are used to verify the performance of our estimation method. Fig.5 shows the scatter plots of estimated Vmax and the Vmax by best track, which distribute near the solid line. The estimated Vmax is perfectly

coincidented with those by the best track, indicating a good estimate. The RMSE of the verification is 13 kt. Hoshino et al.[15] developed a TC intensity estimation method utilizing TRMM/TMI data, with the RMSE being 12 kt over Western North Pacific. Yoshida et al.[16] adopted the same technique of Hoshino to estimate TC intensity using AMSR-E data, with a 11-kt RMSE. The AMSR-E has 6 GHz frequencies the MWRI does not have, and can provide more information. The spatial resolution of TRMM/TMI is higher than that of MWRI. The radiation calibration and space borne instruments vary. All these are possible reasons for the difference between the researches in estimating the intensity of TC. As a result, compared to the 5-kt minimum interval of the best track's Vmax, the result of 13 kt is at the same level of 11-12 kt.

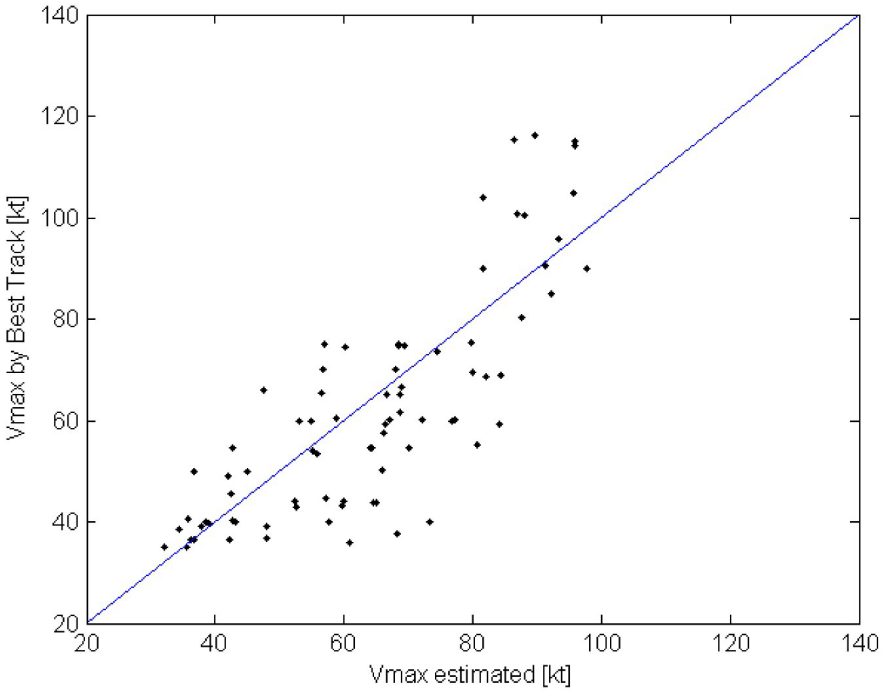

Figure 5. Scatter plots of estimated Vmax and the Vmax by best track.

4 ERROR ANALYSIS

4.1 *Comparison of estimated Vmax by class of best track Vmax*

Statistical research was conducted using the classes of best track Vmax shown in Table 6, and the RMSE and average bias are also given. A large RMSE is seen up to 49 kt and from 90 to 120 kt, which is consistent with the result of Yoshida et al.[16], but the RMSE from 80 to 89 kt is also large, possibly because the sample of this class is too small that its TC characteristics cannot be effectively extracted. Additionally, a reversal of positive and negative average errors takes place on a boundary of around 70 kt, indicating that the estimated Vmax is always stronger below 70 kt but slightly weaker above 70 kt.

Table 6. Comparison of estimated Vmax by class of best track Vmax.

Vmax	Number of cases	Average bias (kt)	RMSE (kt)
Up to 49kt	69	7.4105	12.6842
50–59kt	40	2.4173	9.4664
60–69kt	26	3.5516	10.4381
70–79kt	25	−5.3325	9.5489
80–89kt	10	−5.9718	16.0646
90–120kt	26	−12.7602	16.0694

4.2 *Case study*

An example of time changes for the best track Vmax and estimated Vmax of JELAWAT (the 17th typhoon of 2012) is shown in Fig.6. The time not captured in MWRI images cannot be compared and only a part of whole TC life stages can be seen. The trend of change shows good correspondence, but the estimated Vmax is strong in the early stages of

development and weak toward the mature stage, as compared with the best track Vmax. This matches the comparison of estimated Vmax by the class of best track Vmax, which shows strong estimated Vmax below 70 kt and weak estimated Vmax above it.

Finally, images of cases with large errors were analyzed to find that they are ofen with less organized and asymmetric cloud patterns in the images of 10 GHz (shown in Fig.7). So the classification of TC cloud patterns will help improve the acuracy of the estimated TC intensity further.

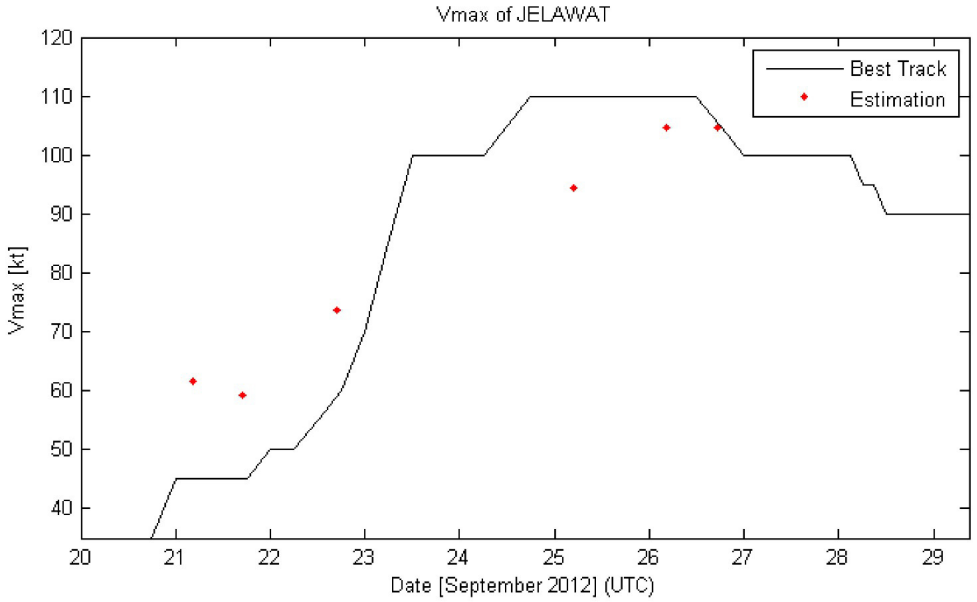

Figure 6. Comparison of time changes between estimated Vmax and best track Vmax.

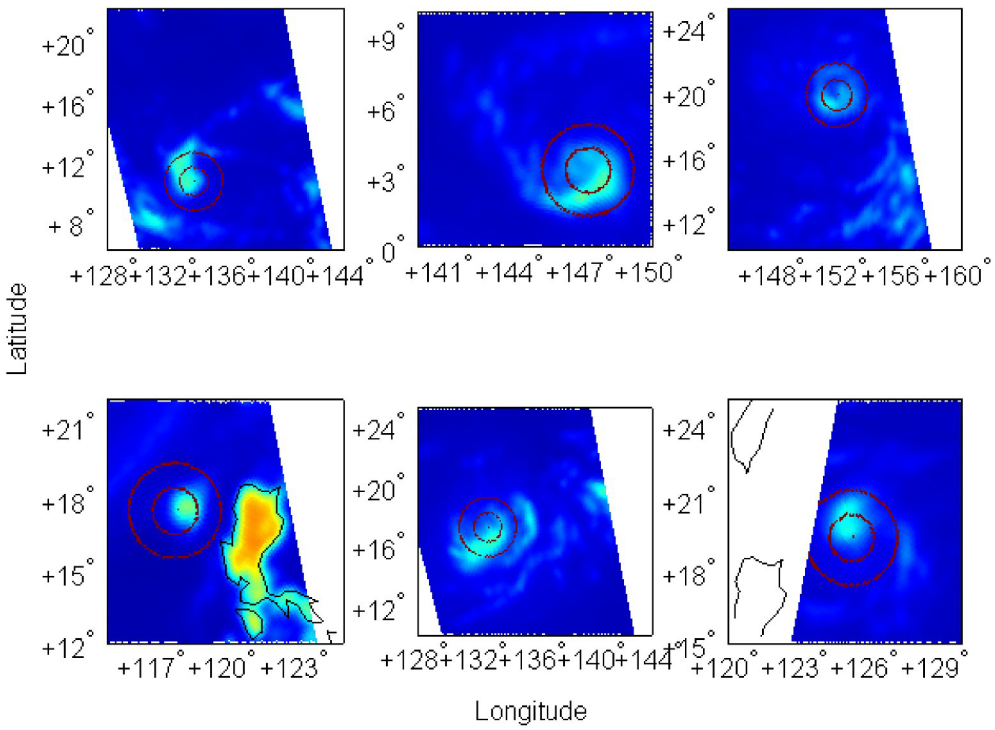

Figure 7. Horizontal polarized TB images at the 10 GHz channel of cases with large bias (Circles are concentric circles whose centers are the ones of the TCs, and the radii are 1° and 2°). (a) ascending orbit on 11 September 2012; (b) descending orbit on 29 November 2012; (c) ascending orbit on 13 July 2011; (d) ascending orbit on 8 December 2012; (e) ascending orbit on 31 July 2011; (f) descending orbit on 20 August 2012.

5 SUMMARY

We developed a method to estimate TC intensity over the Western North Pacific using the FY-3B MWRI data. First, utilizing the data of 2011 and 2012, we investigated the relationship between the FY-3B MWRI TB parameters and the TC Vmax from the best track data. Then by applying PCA and the multiple regression method, an estimation model for estimating TC intensity was established. Finally, utilizing the independent verification data of 2013, the performance of our estimation method was verified. Conclutions are as follows:

(1) The parameters of MIN, MEAN, AREA of lower frequency channels with a radius of 1.0 ° or 1.5 ° from the center give higher correlation, and the highest correlation coefficient is 0.7904.

(2) The estimation model established by applying PCA and multiple regression method shows a good estimate, the RMSE of independent verification is 13 kt.

(3) The estimated Vmax are always strong in the early stages of development, but slightly weaker toward the mature stage, and a reversal of positive and negative bias takes place with a boundary of around 70 kt.

(4) The TC with a larger error ofen has less organized and asymmetric cloud patterns, so the classification of TC cloud patterns will help improve the acuracy of the estimated TC intensity further.

The MWRI of polar-orbit meteorological satellites observe the same location twice a day, and due to the limited observation, the samples with which the estimation model is established are not enough so that some exceptional characteristics of TCs cannot be effectively extracted. Therefore, with the increase of statistical samples the accuracy of the estimated TC intensity will also be improved. In addition, the TC center is obtained from the interpolation of the best track data, therefore if the TC moves irregularly, or its speed changes rapidly, the position of TC may not be accurate. For operational use, we suggest that the infrared image and the results of numerical prediction are used together to determine the TC center, and multi-source data are needed for further improvement.

Also loaded with the MWRI, the FY-3C satellite was launched on september 23, 2013. In the future, TC monitoring by combining daytime and nighttime FY-3C and FY-3B MWRI data is the goal of this research.

REFERENCES:

[1] DVORAK V F. Tropical cyclone intensity analysis and forecasting from satellite imagery [J]. Mon Wea Rev 1975, 103(5): 420-430.

[2] DVORAK V F. Tropical cyclone intensity analysis using satellite data [J]. NOAA Tech Rep NESDIS, 1984, 11: 47.

[3] WANG Jin, JIANG Ji-xi. An objective technique for estimating tropical cyclone intensity from geostationary meteorological satellite observation [J]. J Appl Meteorol Sci, 2005, 16(3): 283-291 (in Chinese).

[4] THOMAS A, JONES, CECIL D. Passive-microwave-enhanced statistical hurricane intensity prediction scheme [J]. Wea Forecast, 2006, 21: 613-635.

[5] LIU Zhe, ZHU Yuan-jing, LI Wan-biao, et al. Development of estimating tropical cyclone intensity with meteorological satellite data [J]. J Trop Meteorol, 2008, 24 (5): 550-556 (in Chinese).

[6] NIU Xiao-lei, LI Wan-biao, Zhu Yuan-jing. Using TRMM data to analyze the relationship between precipitation and water vapor path, latent heat of tropical cyclones [J]. J Trop Meteorol, 2006, 22(2): 113-120 (in Chinese).

[7] WANG Xiao-dan, ZHONG Zhong. Horizontal precipitation structure of AERE (2004) retrieved from TRMM/TMI [J]. J Trop Meteorol, 2007, 23(1): 98-104 (in Chinese).

[8] QIU Hong, FANG Xiang, GU Song-yan, et al. The structure of tropical cyclone from Advanced Microwave Sounding Unit [J]. J Appl Meteorol Science, 2007, 18(6): 810-820 (in Chinese).

[9] KIDDER S Q, GOLDBERG M D, ZEHR R M, et al. Satellite analysis of tropical cyclones using the Advanced Microwave Sounding Unit (AMSU) [J]. Bull Amer Meteorol Soc, 2000, 81(6): 1241-1259.

[10] VELDEN C S, GOODMAN B M, MERRIL T. Western North Pacific tropical cyclone intensity estimation from NOAA polar-orbiting satellite microwave data [J]. Mon Wea Rev, 1991, 119: 159-168.

[11] SPENCER R W, BRASWELL W D. Atlantic tropical cyclone monitoring with AMSU-A:estimation of maximum sustained wind speeds [J]. Mon Wea Rev, 2001, 29(6): 1518-1532.

[12] CECIL D J, ZIPSER E J. Relationships between tropical cyclone intensity and satellite based indicators of inner core convection: 85-GHz ice-scattering and lightning[J]. Mon Wea Rev, 1999, 27: 103-123.

[13] BANKERT R L, TAG P M. An automated method to estimate tropical cyclone intensity using SSM/I imagery [J]. J Appl Meteorol, 2002, 41: 461-472.

[14] LEE T F, TURK F J, HAWKINS J, et al. Interpretation of TRMM TMI images of tropical cyclones [J]. Earth Interact, 2002, 6: 1-17.

[15] SHUNSUKE H,TETSUO N. Estimation of tropical cyclone's intensity using TRMM/TMI brightness temperature data [J]. J Meteorol Soc Jpn. 2007, 85(4): 437-454.

[16] YOSHIDA S, SAKAI M, SHOUJIA, et al. Estimation of Tropical Cyclone Intensity Using Aqua/AMSR-E Data [J]. RSMC Tokyo-Typhoon Center Technical Review, 2011, 13: 1-36.

[17] ZHANG Miao, LU Nai-meng, GU Song-yan, et al. Temperature-sounding microwave channels for FY-3(02) [J]. J Appl Meteorol Sci, 2012, 23 (2): 223-230 (in Chinese).

[18] WENG F, GRODY N. Retrieval of cloud liquid water using the Special Sensor Microwave Imager (SSM/I) [J]. J Geophys Res, 1994, 99(25): 535-551.

[19] YANG Yu-zhen, WANG Yao-ling, HU Bang-hui, et al. An improved statistic-dynamical model for tropical cyclone intensity forecasting in Northwest Pacific [J].

Marine Forecasts. 2010, 27(3): 1-6 (in Chinese).
[20] SONG jin-jie, WANG Yuan, CHEN Pei-yan, et al. A statistical prediction scheme of tropical cyclone intensity over the western north pacific based on the partial least square regression [J]. Acta Meteorol Sinica 2011, 69(5): 745-756 (in Chinese).

Citation: ZHANG Miao, QIU Hong, FANG Xiang et al. Study on the multivariate statistical estimation of tropical cyclone intensity using FY-3 MWRI brightness temperature data [J]. J Trop Meteorol, 2017, 23(2): 146-154.